Plant Physiology and Biochemistry 139 (2019) 44–55

Contents lists available at ScienceDirect

Plant Physiology and Biochemistry

journal homepage: www.elsevier.com/locate/plaphy

Research article

Nitrate supplementation attenuates As(V) toxicity in *Solanum lycopersicum* L. cv Pusa Rohini: Insights into As(V) sub-cellular distribution, photosynthesis, nitrogen assimilation, and DNA damage

Praveen Gupta, Chandra Shekhar Seth*

Assistant Professor, Department of Botany, University of Delhi, Delhi, 110007, India

ARTICLE INFO

Keywords:
As(V)
Ascorbate-glutathione cycle
DNA damage
Nitrate
Nitrogen assimilation
Photosynthesis
Solanum lycopersicum L

ABSTRACT

The present study investigates As(V) toxicity in tomato (*Solanum lycopersicum* L. cv Pusa Rohini) and its alleviation by exogenous supplementation of nitrate. The seven days old seedlings were grown up to thirty days under defined levels of As(V) concentrations (0, 2.5, 6.25, and 12.5 mg/250 g soil) in alone or/and in combination with 20 mM nitrate. The arsenic accumulation, lipid peroxidation, DNA damage, photosynthesis, nitrogen assimilation, and AsA-GSH cycle were evaluated. Results revealed that As(V) exposure significantly ($P \leq 0.05$) enhances the root, leaf and leaf sub-cellular arsenic accumulation, H_2O_2 and MDA contents in a dose-dependent manner. Comet assay indicated a progressive enhancement in the DNA damage with maximum tail length (58.33 ± 9.87 µm) and tail moment (25.05 ± 2.80) at 12.5 As(V) exposure. Nitrate supplementation counteracted As(V) toxicity on photosynthesis, nitrogen assimilation, and boosts AsA-GSH cycle at each respective As (V) treatments. The net photosynthesis was increased by 18% at 6.25 As(V), however, stomatal conductance and F_v/F_m were increased by 26%, and 11%, respectively, at 2.5 As(V) exposure. The activities of NR and GS were enhanced by 29% and 18%, respectively; contents of NO_3^-, NO_2^- and NH_4^+ were improved by 21%, 56%, and 13%, respectively, at 6.25 As(V) exposure. The activities of APX and GR were increased concomitantly with the ratios of AsA/DHA and GSH/GSSG. The study demonstrates that nitrate supplementation significantly ($P \leq 0.05$) decreases As(V) accumulation, boosts the performance of AsA-GSH cycle, and consequently enhances the photosynthesis and nitrogen assimilation. Based on present findings, nitrate supplementation could be recommended as a promising approach to ameliorate the As(V) toxicity in plants.

1. Introduction

Arsenic (As) is a highly toxic and carcinogenic metalloid, naturally present in low to high amounts in the environment. It ubiquitously occurs in the rocks and is naturally distributed in the soil and water by geochemical events like weathering of rocks and volcanic emissions (Shakoor et al., 2016). However, anthropogenic activities such as industrialization, mining, coal combustion, smelting and use of As enriched preservatives, insecticides and herbicides considerably enhance As contamination in the environment (Niazi et al., 2017). Arsenic contamination has become a global risk as it readily enters in the ecological food chain and affects human health through biomagnification. It commonly exists in two inorganic forms *viz* trivalent arsenite [As(III)] and pentavalent arsenate [As(V)] of which former has better mobility and hence is more toxic (Mehmood et al., 2017). In root cells, As(III) transport is mediated by aquaporins channels, while As(V) is transported via phosphate transporters. Once taken up by the plant cells, As(V) rapidly converted to As(III) by arsenate reductase (AR) and subsequently the As(III) binds with glutathione (GSH) and phytochelatins (PCs) to make As(III)-thiols complex. The sequestration of As(III)-thiols complex into the vacuole of root cells is crucial for As(III)-detoxification and restricting its long-distance transport to the other tissues in the plants (Abbas et al., 2018). The accumulation of As in plant tissues and sub-cellular distribution are closely linked to its phytotoxicity as it readily binds with sulfhydryl (—SH) groups of proteins and impairs the DNA repair enzymes. It also replaces the phosphorus from DNA, thus distorts the DNA stability (Abbas et al., 2018). Arsenic damages the histone proteins and forms the As-DNA adducts that generate the DNA fragments and DNA or DNA-protein cross-links (Chandrakar et al., 2017; Abbas et al., 2018). Several phytotoxic effects of As are reported on nutrients uptake, leaf gaseous exchange, photosynthetic pigments, and nitrogen assimilation (Rafiq et al., 2017; Singh et al.,

---

* Corresponding author.
E-mail addresses: csseth52@gmail.com, seth_bhu@yahoo.co.in (C.S. Seth).

https://doi.org/10.1016/j.plaphy.2019.03.007
Received 5 February 2019; Received in revised form 5 March 2019; Accepted 5 March 2019

2018c).

The availability of plant nutrients has recently gained importance in minimizing the phytotoxicity of heavy metals including As(V) and nitrate has a driving role in the regulation of nitrogen metabolism and photosynthesis (Singh et al., 2016b, 2018c). Nitrogen supplementation has shown positive impacts under abiotic stresses as it constitutes the backbone of amino acids, proteins, nucleic acids, vitamins, chlorophyll, and antioxidants (Krapp, 2015). In soil solution, nitrate and ammonium represent the two common forms of inorganic nitrogen and their uptake is mediated by nitrate transporters (NRT) and ammonium transporters (AMT), respectively (Krapp, 2015). Nitrogen assimilation involves the conversion of nitrate to ammonium by sequential actions of NR and NiR. After direct uptake or conversion from nitrate, ammonium is assimilated to glutamine and glutamate by GS-GOGAT or GDH cycle (Singh et al., 2016b; Gupta et al., 2017). The photosynthesis and nitrogen metabolism have an intimate relationship as (i) proteins of the Calvin cycle and thylakoids represent majority of the leaf nitrogen (Zhong et al., 2018a) and (ii) photosynthetic electron transport chain donates electrons for NO_2^- reduction via ferredoxin for NiR activity. It has been reported that nitrogen availability enhances the photosynthesis by increasing the chlorophyll biosynthesis, gaseous exchanges and stomatal movement under the stress conditions (Zhong et al., 2017, 2018a).

Ascorbate-glutathione (AsA-GSH) cycle is an important mechanism to avert the oxidative damages in different sub-cellular compartments. It includes both enzymatic (APX, DHAR, MDHAR, GR) and non-enzymatic (AsA, DHA, GSH, GSSH) antioxidants. Ascorbate peroxidase (APX) and Glutathione reductase (GR) are two key enzymes of the cycle as APX directly involves in H_2O_2 detoxification, and GR regenerates GSH from GSSG at the expense of NADPH to maintain a high GSH/GSSG ratio (Noctor et al., 2016). Glutathione is a decisive factor as it regenerates the AsA and ensures the continuous running of the cycle (Farooq et al., 2018). This cycle potentially scavenges ROS and protects from their severe consequences on vital plants' metabolic processes like photosynthesis, nitrogen metabolism and DNA damage under various abiotic stresses (Zhong et al., 2018a; Farooq et al., 2018).

Tomato (*Solanum lycopersicum* L.) is an important vegetable crop and occupies a unique position in the human diet due to its richness in vitamins, mineral nutrients, tocopherols, polyphenols, antioxidants, and lycopene. In the backdrop of increasing human demands under unprecedented population rise, it is a great challenge for scientists to combat the loss in tomato production growing under As-contaminated soil. Therefore, it is imperative to devise our approach that can efficiently restrict and minimize the phytotoxic effects of As(V) without compromising with the soil fertility. The present study was carried out to explore the possible mechanism(s) of nitrate mediated alleviation of As(V) toxicity by analyzing the As(V) accumulation in root, leaf, and in leaf subcellular fractions, lipid peroxidation, DNA damage, photosynthesis, nitrogen assimilation, and AsA-GSH cycle. Numerous studies have been carried out to examine the ameliorative effects of nitrate under various abiotic stresses. However, few reports are available on nitrate mediated amelioration of As(V) toxicity in tomato plants. Nitrate supplementation proved to be a feasible and promising approach for the enhancement of tomato growth by minimizing the As uptake and improving the AsA-GSH cycle, photosynthesis and nitrogen assimilation.

2. Materials and methods

2.1. Plant material, growth conditions and As(V) exposure to plants

The tomato seeds were procured from the Indian Agricultural Research Institute (IARI), New Delhi, India. Seven days old uniform sized seedlings were transplanted in plastic pots (13 cm diameter) containing 250 g soilrite (perlite + irish peat moss + vermiculite) and garden soil mixture with a range of As(V) [0, 2.5, 6.25 and 12.5 mg] with or without 20 mM nitrate. The As(V) was applied as disodium hydrogen arsenate ($Na_2HAsO_4.7H_2O$) and potassium nitrate (KNO_3) was used as a source of nitrate. The plants were grown in a triplicate manner with each pot containing three seedlings (nine plants per treatment). The pots were kept in the net house of Department of Botany, University of Delhi, India, and seedlings were grown up to one month under natural environmental growth conditions (mean temperature, 23 ± 2 °C). The drainage of soil solution was prevented by irrigating slightly lesser than the field capacity. After the termination of the experiment, the plants were carefully uprooted (between 10:00 and 12:00 a.m.) and plant organs (root and leaves) were manually separated. The upper fully-expanded young leaves and whole roots were rinsed briefly (3–4 times) in deionized water and immediately submerged in liquid N_2, and stored at −80 °C for DNA damage and biochemical analysis. Separated leaf and root samples were dried in hot air oven at 65 °C for 2–3 days till constant weight achieved.

2.2. Extraction and quantification of As(V) in root, leaf, and leaf subcellular fractions

Dried and finely powdered root and leaf samples were acid digested [HNO_3:$HClO_4$, (3:1,v/v)], filtered and diluted up to 50 mL by double-distilled water. The samples were analyzed for Arsenic quantification by using the atomic absorption spectrometer (Perkin-Elmer; Analyst 600, U.S.A).

For determination of arsenic subcellular accumulation, fresh leaf samples (1 g) were homogenized in pre-cold extraction buffer containing 50 mM Tris-HCl (pH 7.5), 0.25 M sucrose and 1 mM DTT and the different fractions were isolated by differential centrifugation technique (Farooq et al., 2016). The homogenate was centrifuged at 3000 rpm for 15 min (4 °C) and the precipitated residue was designated as cell wall fraction (F1). The supernatant fraction was further centrifuged at 15,000 rpm for 30 min (4 °C) and the obtained supernatant and residue were considered as soluble fraction (F2) and organelles fraction (F3), respectively. The separated fractions were acid digested, diluted to 25 mL using deionized water and used for arsenic content determination.

2.3. Determination of H_2O_2 content and lipid peroxidation

Leaf samples (500 mg) were homogenized in 2.5 mL of 0.1% TCA (w/v) and centrifuged at 10,000 × g for 20 min at 4 °C. The supernatant (0.5 mL) was mixed with 0.1 M phosphate buffer (pH 7.6) and 1 M potassium iodide (Alexieva et al., 2001). After 1 h incubation in dark, the absorbance of reaction mixture was recorded at 390 nm and H_2O_2 content was determined by using a standard curve of hydrogen peroxide.

The degree of lipid peroxidation was assessed by determining the malondialdehyde (MDA) content. Briefly, leaf samples (100 mg) were homogenized in 1% (w/v, TCA) and centrifuged at 10,000 × *g* for 15 min. The supernatant (1 mL) was mixed with 4 mL of thiobarbituric acid (TBA) reagent (20% TCA containing 0.5% of TBA) and the reaction mixture was incubated at 95 °C (30 min) in a water bath (Heath and Packer, 1968).

2.4. Comet assay (single cell gel electrophoresis)

The nuclei were isolated under the dim yellow light in a petri dishes containing ice-cold 400 mM Tris buffer (pH 7.5). The comet slides prepared by scratching the glass slides with the diamond knife and sinking into 1% aqueous normal melting agarose (NMP) solution. Onto each NMP agarose coated slide, 100 μL each of nuclear suspension and 1% low melting agarose (LMA) were added and slides were allowed to cool on ice after placing the coverslip. The slides were coated with an additional layer of 0.5% LMP agarose (100 μL) and dipped in a horizontal gel-electrophoresis tank containing cold electrophoresis buffer

[300 mM NaOH containing 1 mM Na_2EDTA (pH > 13)]. The electrophoresis was performed at 26 V, 300 mA for 30 min at 4 °C. After electrophoresis, slides were gently rinsed with 400 mM Tris buffer (pH 7.5) and stained with ethidium bromide (20 µg mL^{-1}). The comets were observed under fluorescence microscope enabled with an excitation filter of BP 546/10 nm and a barrier filter of 590 nm (Gichner et al., 2016). The tail length and olive tail moment were determined by using the CASP software.

2.5. Analysis of photosynthetic attributes under As(V) exposure and nitrate supplementation

2.5.1. Scanning electron microscopy of leaf epidermal and guard cells

The fine sections of leaf samples (1 mm^2) were fixed in Karnovsky fixative followed by dehydration in 25%, 50%, 75%, and 100% ethanol (for 30 min each) gradient series and then subjected to critical point drying (Gupta et al., 2017). The samples were coated with a layer of gold-palladium and observed under the Scanning electron microscope (JEOL- JSM-6610LV, Japan). Minimum 6 SEM images per plant (12 pictures per replicate) were taken for the assessment of structural anomalies in leaf epidermal and guard cells.

2.5.2. Leaf gas exchange parameters and chlorophyll fluorescence

The leaf gas exchange parameters (A, GH_2O) were measured on fully expanded young leaves using portable open system Infra Red Gas Analyzer (IRGA, Gas Exchange Fluorescence System, GFS-3000, Germany) between 9.00 a.m. and 12.00 noon. Before taking final observations, the IRGA was calibrated for ambient CO_2 concentration (~398 ppm), photosynthetic photon flux density (750 µmol m^{-2} s^{-1}), cuvette temperature 25 °C, impeller at 7, and relative humidity inside the cuvette at ~53%. The air humidity in the location where the experiment conducted was ~60%. The half leaf portion was inserted in a leaf chamber and the final observations were recorded. The F_v/F_m values were calculated in dark-adapted leaves (30 min) by changing the module of IRGA to fluorescence.

2.5.3. Photosynthetic pigments contents

Photosynthetic pigments (Chlorophyll *a*, *b*) and carotenoids were extracted in 100 mg of fresh leaves homogenized in 7 mL of DMSO and incubated at 60 °C for 20 min. The DMSO (3 mL) added again to maintain the final volume to 10.0 mL (Hiscox and Israelstam, 1979). The absorbance of the supernatant was recorded at 452.5, 645, 663 nm (UV–visible spectrophotometer, Beckman Coulter DU 730, U.S.A) to calculate the photosynthetic pigments.

2.5.4. Carbonic anhydrase activity and photosynthates contents

Frozen leaves (100 mg) were homogenized in 20 mM Tris- HCl buffer (pH 8.3) containing 10 mM 2-mercaptoethanol and 1 mM EDTA. The homogenate was centrifuged at 15,000 × *g* (4 °C) and the extract proceeded for activity determination. The enzyme extract (100 µL) was added to 6 mL of 20 mM Tris-HCl buffer (pH 8.3), and the reaction was initiated by adding 4 mL of ice-cold CO_2 saturated water. The time required for pH drop from 8.3 to 6.3 in the presence (Ts) and absence (T_0) of the enzyme was recorded using pH-meter (Eutech, Singapore) and the enzyme activity calculated by applying the formula: Units g^{-1} FW = $2(T_0 - T_s)/T_0$ [g FW] (Singh et al., 2016b).

Dried leaves (200 mg) were homogenized in 8 mL of 80% ethanol (v/v), and centrifuged (3000 × *g* for 10 min) to collect the supernatant and pellet. The process was repeated three times and the supernatants were pooled and made up to 50 mL using 80% ethanol. The supernatant was used for sucrose and the pellet was for starch determination. The reaction mixture for sucrose content determination contains 1 mL of extract, 1 mL 15% phenol and 5 mL of conc. H_2SO_4 (Buysse and Merckx, 1993). Starch was extracted from the pellet using 52% perchloric acid and the content was determined using the anthrone reagent at 630 nm (Clegg, 1956).

2.6. Analysis of nitrogen assimilation under As(V) exposure and nitrate supplementation

2.6.1. Nitrate, nitrite and ammonium contents

For nitrate, nitrite and ammonium contents estimation, dried and finely powdered leaves samples (50 mg) were acid digested, filtered and maintained to 50 mL using double distilled water. The reaction mixture for nitrate content estimation consisted of 100 µL filtrate and 200 µL of 5% salicylic acid (Cataldo et al., 1975). The reaction was terminated after 15 min by adding 1 mL of 4 M NaOH and the absorbance recorded at 410 nm. The nitrate content was calculated by using a standard curve of KNO_3.

Nitrite content was determined in a reaction mixture containing 1 mL of the supernatant, 2 mL of 1% (w/v) sulfanilamide, and 2 mL of 0.02% (w/v) of N-(1-naphthyl) ethylenediamine dihydrochloride (Varner et al., 1953). The absorbance was recorded at 520 nm and nitrite content was determined by using a standard curve of $NaNO_2$.

Ammonium content was determined in a reaction mixture containing 100 µL supernatant, 10 µL 10% K—Na tartrate, 2.4 mL double distilled water, and 100 µL Nessler's reagent (Molins-Legua et al., 2006). The absorbance was measured at 425 nm and ammonium content was calculated using a standard curve of NH_4Cl

2.6.2. Nitrogen assimilating enzymes assay

Nitrate reductase (NR, EC 1.7.99.4) activity was determined as earlier (Gupta et al., 2017). The enzyme extract was added to 1% sulphanilamide and 0.02% N-(1-naphthyl)-ethylenediamine dihydro chloride-HCl (NED-HCl) and the absorbance was recorded at 540 nm using spectrophotometer. The activity was determined by using a KNO_2 standard and expressed in µmol NO_2^- produced h^{-1} g^{-1} fresh weight.

Nitrite reductase (NiR, EC 1.7.2.1) assay reaction mixture consisted of 50 mM Tris-HCl buffer (pH 7.5), 0.1 mM NADPH, 0.1 mM KNO_2, 0.01 mM FAD^+ and enzyme extract (Sengupta and Shaila, 1996). The disappearance of NADPH was recorded at 340 nm. The NiR activity was determined by using KNO_2 as a standard and expressed in µmol NO_2^- disappeared h^{-1} g^{-1} fresh weight.

Glutamine synthetase (GS; EC 6.3.1.2) activity assay reaction mixture consisted of 100 mM Tris-HCl buffer (pH 7.9), 60 mM hydroxylamine hydrochloride, 10 mmol glutamine, 20 µM disodium hydrogen arsenate, 50 µM ATP, 1 µM $MgCl_2$, and the aliquot of enzyme extract. After 30 min incubation at 37 °C, the reaction was terminated by adding freshly prepared 2 mL of $FeCl_3$ reagent (equal volumes of 0.57 M $FeCl_3$, 1 M HCl, 0.5 M trichloroacetic acid). The absorbance was recorded at 540 nm and GS activity expressed in µmol γ-glutamyl hydroxamate produced $min^{-1}g^{-1}$ fresh weight (O'neal and Joy, 1973).

Glutamine-2-oxoglutarate aminotransferase (NADH-GOGAT; EC 1.4.1.14) activity assay reaction mixture consisted of 5 mM α-oxoglutaric acid, 10 mM glutamine and 0.15 mM NADH in 50 mM phosphate buffer (pH 7.5) and the enzyme extract. The oxidation of NADH was recorded at 340 nm for 3 min and the activity expressed in µmol NADH oxidized h^{-1} g^{-1} fresh weight (Rachim and Nicholas, 1985).

2.7. Determination of enzymatic and non-enzymatic antioxidants of AsA-GSH cycle

2.7.1. APX and GR activities

Leaf samples (150 mg) were homogenized in extraction buffer containing 50 mM potassium phosphate buffer (pH 7.8) containing 0.1 mM EDTA, 2 mM AsA and 2% (w/v) polyvinyl pyrrolidone 0.1 mM EDTA. The homogenate was centrifuged at 10,000 × *g* for 20 min at 4 °C, and the collected supernatant was used for analysis of APX and GR activity (Noctor et al., 2016). The reaction mixture (1 mL) for APX assay contained 10 mM ascorbate, 100 mM phosphate buffer (pH 7.5), 1 mM EDTA, and the aliquot of the enzyme extract. The reaction was initiated by adding 0.2 mM H_2O_2 and the decrease in absorbance recorded at 290 nm. The APX activity was calculated using a molar extinction coefficient (2.8 $mM^{-1} cm^{-1}$) and expressed as mmol Vit. C min^{-1} g^{-1} FW. The GR activity was determined in a reaction mixture consisted of 100 mM potassium phosphate buffer (pH 7.0) containing 1.0 mM EDTA, 10 mM NADPH and the aliquot of enzyme extract. The reaction initiated by adding 50 mM oxidized glutathione (GSSG) and the decrease in absorbance was recorded at 340 nm. GR activity was calculated using a molar extinction coefficient (6.20 $mM^{-1} cm^{-1}$) and expressed as μmol NADPH min^{-1} g^{-1} FW.

2.7.2. Ascorbate and glutathione contents

The supernatant for AsA and GSH contents determination was prepared by homogenizing the leaf samples (500 mg) in 5% (w/v) TCA followed by centrifugation at 10,000 × *g* for 15 min at 4 °C (Wu et al., 2006). The reaction mixture for AsA determination consisted of 100 mM phosphate buffer (pH 7.7), 10% (w/v) TCA, 4% (w/v) 2, 2′-bipyridyl, 44% (v/v) H_3PO_4, 3% (w/v) $FeCl_3$, and the supernatant. The absorbance of the colored reaction was recorded at 525 nm. For determining the total AsA content 0.2 mM DTT was added to the aforesaid reaction mixture. The DHA content was derived as a difference of the total AsA and AsA.

The reaction mixture for GSH content estimation consisted of 100 mM phosphate buffer (pH 7.7), 0.6 mM DTNB and the supernatant. The reaction mixture was incubated at room temperature for 30 min and the absorbance was recorded at 412 nm. The total GSH content was determined in the same reaction mixture containing an additional 1 unit GR and 0.15 mM NADPH. The GSSG content was derived as a difference of total GSH and GSH.

3. Statistical analysis

The experimental data is a mean of three biological and three technical replicates. The data is processed by using the Microsoft Excel 2010 and represented as mean ± standard error. Statistical analysis was performed by two way ANOVA analysis to assess the effect of nitrate and arsenic and the interaction, followed by Duncan's multiple range test to compare between all the treatments using the SPSS software version 21.0. (SPSS, Chicago, USA) at $P \leq 0.05$.

4. Results

4.1. As(V) accumulation in root, leaf and in leaf subcellular fractions of plants grown under As(V) exposure and nitrate supplementation

The differential accumulation of As(V) in roots, leaves and leaf sub-cellular fractions is presented in Table 1. Arsenic was undetectable in the plants grown in control and nitrate alone treatments. The As accumulation in both roots and leaves significantly ($P \leq 0.05$) increased with the As concentrations in the soil with a higher magnitude reported in roots as compared to the leaves. Nitrate supplementation significantly ($P \leq 0.05$) lowered the As content in roots and leaves under arsenic stress. At 12.5 As(V) treatment, roots and leaves accumulated 873.97 ± 7.76 and 218.73 ± 3.88 μg kg^{-1} DW arsenic, respectively, while nitrate co-application lowered it in both roots (688.47 ± 3.37 μg kg^{-1} DW) and leaves (181.05 ± 2.65 μg kg^{-1} DW). For leaf sub-cellular fractions i.e. cell wall (F1), soluble (F2) and organelles fraction (F3) arsenic accumulation exhibited the similar pattern to that of root and leaves. In sub-cellular fractions, the arsenic sub-cellular accumulation followed F1>F2>F3 pattern. However, nitrate supplementation under As(V) stress effectively lowered the As(V) accumulation in all three fractions as compared to their As(V) alone counterparts. Two-way anova analysis showed that arsenic accumulation was significantly ($P \leq 0.05$) affected by arsenic, nitrate and their interaction. At 6.25 and 12.5 As(V) alone treatments, the As contents in cell wall fraction were 70.16 ± 2.23 and 86.17 ± 11.32 μg kg^{-1} DW, respectively, while at each respective nitrate treatment the deposition lowered to 31.74 ± 0.072 and 61.15 ± 6.51 μg kg^{-1} DW, respectively.

4.2. H_2O_2 and lipid peroxidation

A significant ($P \leq 0.05$) enhancement in the contents of H_2O_2 and malondialdehyde (MDA) were observed upon As(V) exposure as compared to the control. The H_2O_2 content increased by 15%, 50% and 117%, respectively, at 2.5, 6.25 and 12.5 As(V) as compared to the control, however, nitrate supplementation curbed the H_2O_2 by 6%, 9%, and 10%, respectively, as compared to their As(V) alone counterparts (Fig. 1A). The MDA content increased by 3.8 fold and more than 7.0 fold at 6.25 and 12.5 As(V), respectively. By contrast, nitrate supplementation decreased the MDA content at each respective As(V) alone treatment (Fig. 1B). A two-way ANOVA analysis showed that MDA content was significantly affected by arsenic (F = 2117.78, P = 0.000), nitrate (F = 256.97, P = 0.000), and their interaction (F = 64.46, P = 0.000; Table 6).

4.3. DNA damage under As(V) exposure and nitrate supplementation

The cellular comet assay revealed significant ($P \leq 0.05$) enhancements in the tail length (TL) and olive tail moment (OTM) under As(V) stress. The lowest As(V) exposure did not induce severe DNA damage, however, 6.25 and 12.5 As(V) treatments aggravated the DNA damage (Fig. 2A–C). The DNA tail length increased from 6.0 ± 1 [2.5 As(V)] to 58.33 ± 9.87 μm [12.5 As(V)] and OTM values from 0.698 ± 0.18 [2.5 As(V)] to 25.05 ± 2.81 [12.5 As(V)]. By contrast, the nitrate supplementation showed ameliorative effects and lowered the DNA damage as compared to the respective As(V) alone treatments. The TL values range from 4.67 ± 0.58 [2.5 As(V) + nitrate] to 20.66 ± 4.04 [12.5 As(V) + nitrate], whereas OTM from 0.51 ± 0.06 [2.5 As(V) + nitrate] to 4.39 ± 0.42 [12.5 As(V) + nitrate]. A two-way ANOVA analysis revealed that tail length and olive tail moment were significantly affected by As(V), nitrate, and their interaction (Table 6).

Table 1

Quantification of As(V) accumulation in root, leaf, and leaf-subcellular distribution in cell wall (F1), soluble (F2) and organelles (F3) fractions from *Solanum lycopersicum* L. grown under various As(V) treatments and 20 mM nitrate supplementation. Data is presented as mean ± S.E (n = 3). Different lower case letters indicate significant differences among the treatments as per Duncan's test.

	Accumulation of Arsenic (μg Kg^{-1} DW)		Leaf sub-cellular distribution of Arsenic (μg Kg^{-1} FW)		
Treatments	Root	Leaf	Cell wall	Soluble	Organelles
Control	Nd	Nd	Nd	Nd	Nd
NO_3^-	Nd	Nd	Nd	Nd	Nd
2.5 As(V)	555.20 ± 1.95^d	129.39 ± 6.16^c	55.23 ± $3.05^{c,d}$	38.89 ± 2.05^c	6.71 ± 0.38^e
2.5 As(V) + NO_3^-	424.17 ± 3.36^e	72.98 ± 6.14^e	44.77 ± 4.25^d	Nd	Nd
6.25 As(V)	734.95 ± 3.00^b	172.53 ± 4.73^b	70.16 ± 2.23^b	48.04 ± 1.98^b	40.84 ± 1.81^b
6.25 As(V) + NO_3^-	555.41 ± 2.21^d	94.94 ± 5.35^d	31.74 ± 0.072^e	25.91 ± 2.51^d	18.67 ± 0.81^d
12.5 As(V)	873.97 ± 7.76^a	218.73 ± 3.88^a	86.17 ± 11.32^a	73.22 ± 3.54^a	52.50 ± 5.87^a
12.5 As(V) + NO_3^-	688.47 ± 3.37^c	181.05 ± 2.65^b	61.15 ± $6.51^{b,c}$	41.46 ± 2.70^c	27.81 ± 5.24^c

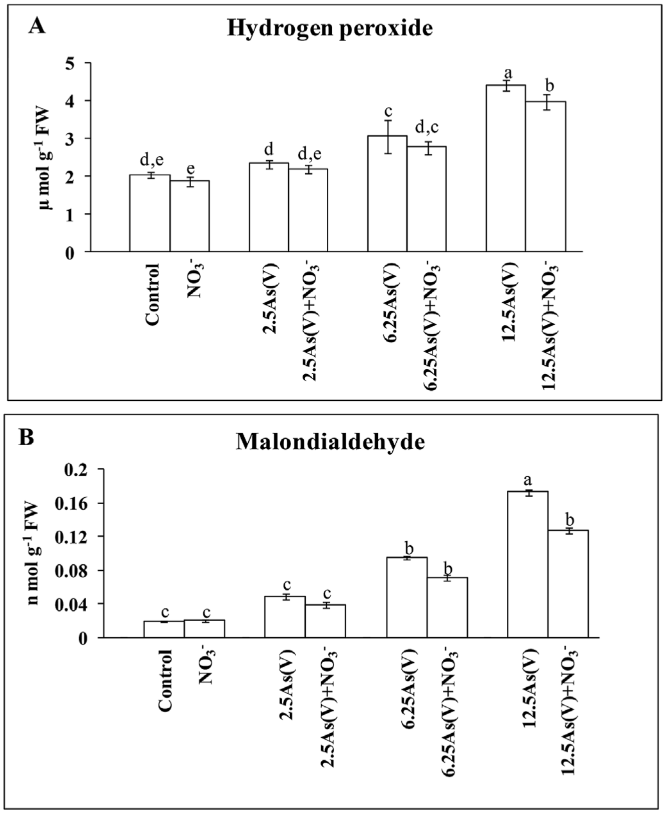

Fig. 1. (A) Hydrogen peroxide and (B) Malondialdehyde content in the leaves of *Solanum lycopersicum* L. grown under various As(V) treatments and 20 mM nitrate supplementation. Data is presented as mean ± S.E (n = 3). Different lower case letters indicate significant differences among the treatments as per Duncan's test.

4.4. Photosynthetic performance under As(V) exposure and nitrate supplementation

4.4.1. Structural anomalies in leaf epidermal and guard cells

The SEM images revealed that As(V) exposure largely deteriorated the shape of the guard and leaf epidermal cells. The stressed leaves showed distorted, shrunk epidermis and closed stomata with distorted guard cells. At the highest As(V) exposure, guard cells were seen completely fused with epidermal cells, however, under nitrate supplementation epidermal and guard cells showed relatively improved shape and structure (Fig. 3).

4.4.2. Leaf gas exchange parameters, chlorophyll fluorescence, and photosynthetic pigments

The net photosynthetic rate (A), stomatal conductance (GH_2O), and chlorophyll fluorescence (F_v/F_m) were deteriorated by 51%, 35%, and 13%, respectively, under the 12.5As(V) exposure. However, nitrate supplementation improved the aforesaid parameters by 17%, 31%, and 13%, respectively, as compared to the 12.5As(V) alone treatment. The chlorophyll *a, b* and carotenoids contents were decreased by 69%, 72%, and 67%, respectively under 12.5 As(V) alone treatment as compared to the control (Table 2). However, nitrate supplementation significantly ($P \leq 0.05$) increased the photosynthetic pigments contents than their respective As(V) alone treatments. The maximum enhancement in chlorophyll *a, b* and carotenoids contents were 59%, 58%, and 97%, respectively than the respective 2.5 As(V) alone treatment. A two way ANOVA analysis showed that A, GH_2O, F_v/F_m, and photosynthetic pigments were significantly ($P \leq 0.05$) affected by As(V), nitrate, and their interaction (Table 6).

4.4.3. Carbonic anhydrase activity and photosynthates contents

The decrease in carbonic anhydrase (CA) activity and photosynthates (starch, and sucrose) contents were directly related to the As (V) levels in the soil. Nitrate supplementation enhances the CA activity, starch, and sucrose contents more effectively at 2.5 As(V) treatment and to a lesser extent at higher treatments. The CA activity, starch, and sucrose contents were reduced by 43%, 38%, and 68%, respectively, at 12.5As(V) treatment (Table 3) as compared to the control. Furthermore, nitrate supplementation improved the aforesaid parameters by 18%, 13%, and 13%, respectively, as compared to 12.As(V) alone counterpart. A two way ANOVA analysis revealed that CA activity, starch, and sucrose contents were significantly ($P \leq 0.05$) affected by As(V), and nitrate treatments; contrarily the interaction between As(V) and nitrate was non-significant for CA activity and starch contents (Table 6).

4.5. Inorganic nitrogen contents and nitrogen assimilating enzymes under As(V) exposure and nitrate supplementation

4.5.1. Inorganic nitrogen contents

The nitrate, nitrite, and ammonium contents were significantly ($P \leq 0.05$) declined by 47%, 59%, and 40%, respectively, at 12.5 As(V) treatment as compared to the control (Table 4). However, nitrate supplementation enhanced the NO_3^-, NO_2^- and NH_4^+ contents in alone and under As(V) stress. The 6.25 As(V) + nitrate treatment generated the best response and enhanced the NO_3^- and NO_2^- contents by 21% and 57%, respectively, as compared to 6.25 As(V) alone treatment. A two-way ANOVA analysis showed that nitrate, nitrite, and ammonium contents were significantly ($P \leq 0.05$) affected by As(V) and nitrate treatments, however, the interaction between As(V), and nitrate was non-significant for nitrite, and ammonium contents (Table 6).

4.5.2. Nitrogen assimilating enzymes

The activities of nitrate (NR and NiR) and ammonium (GS and GOGAT) assimilating enzymes were significantly ($P \leq 0.05$) decreased under As(V) stress (Fig. 4A–D). The decline in NR activity was 16%, 47%, and 56%, whereas NiR activity decreased by 16%, 47%, and 56% with 2.5, 6.25 and 12.5 As(V) treatments, respectively, in comparison to the control. The decrease in GS activity was 8% and 29% and the corresponding decrease in GOGAT was 43% and 56% at 6.25 and 12.5 As(V) treatments, respectively. Nitrate supplementation improved NR, NiR, GS and GOGAT activities as compared to the activities recorded under 2.5, 6.25 and 12.5 As(V) alone treatments. The two-way ANOVA analysis did not reveal any significant ($P \leq 0.05$) interactions between As(V) and nitrate treatments for NR, NiR, and GOGAT activities (Table 6).

4.6. Enzymatic and non-enzymatic antioxidants of AsA-GSH cycle

The APX and GR activities were increased at 2.5 As(V), whereas showed inhibition at 6.25 As(V) and 12.5 As(V) treatments. The activities of APX and GR were increased by 79% and 31%, respectively, at 2.5 As(V), while further declined by 54% and 39%, respectively, at 12.5 As(V) treatment as compared to the control. Nitrate supplementation boosts the APX and GR activities as compared to respective As(V) alone counterparts. At 12.5 As(V) alone treatment, nitrate supplementation improved the APX and GR activity by 51% and 9%, respectively, as compared to 12.5 As(V) alone counterpart (Fig. 5A and B). A two-way ANOVA analysis showed that APX and GR activities were significantly ($P \leq 0.05$) affected by As(V), nitrate, and their interactions (Table 6). The non-enzymatic antioxidants *viz.* AsA, DHA, GSH, GSSG, exhibited an interesting pattern. The antioxidants contents showed a gain at 2.5 and 6.25 As(V), while decreased at 12.5 As(V) exposure as compared to the control plants. The plants exposed to 2.5 As(V) increased the AsA content and AsA/DHA ratio by 48% and 34%, and the corresponding increase in GSH content and GSH/GSSG ratio was 61% and 27%, respectively, as compared to the control. Furthermore, nitrate

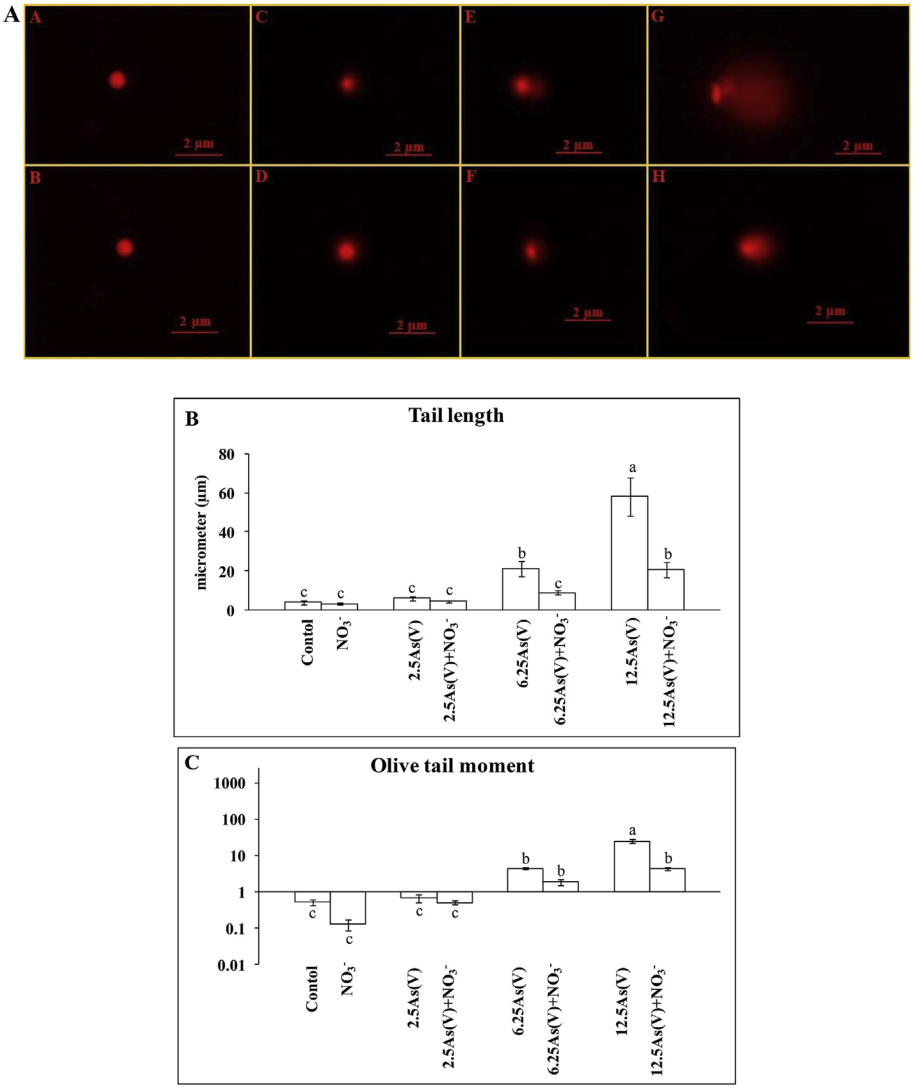

Fig. 2. (A) Comet images, (B) tail length, and (C) olive tail moment of leaf nuclei of 30 days old *Solanum lycopersicum* L. illustrating the degree of DNA damage at various As(V) treatments and its recovery up to the certain extent at each nitrate counterparts. (A = Control, B = 20 mM nitrate, C = 2.5 As(V), D = 2.5 As(V) + 20 mM nitrate, E = 6.25 As(V), F = 6.25 As(V) + 20 mM nitrate, G = 12.5 As(V), H = 12.5 As(V) + 20 mM nitrate).

supplementation to the As(V) stressed plants resulted in the improvement of AsA, AsA/DHA, GSH, and GSH/GSSG as compared to their alone counterparts (Table 5). A two-way ANOVA analysis did not reveal any significant ($P \leq 0.05$) interactions between As(V) and nitrate treatments with respect to AsA, AsA/DHA, GSH, GSSG, and GSH/GSSG (Table 6).

5. Discussion

5.1. As(V) accumulation, lipid peroxidation and DNA damage under As(V) exposure and nitrate supplementation

Arsenic is a toxic metalloid and has no known essential function in promoting the plant growth (Mehmood et al., 2017). In the present study, a dose-dependent enhancement of As(V) accumulation was observed in both roots and leaves (Table 1). The arsenic uptake is largely governed by As concentration gradient between soil and plant cells (Abbas et al., 2018). It is reported that phosphate (Pi) transporters facilitated As(V) uptake as the oxyanion chemical structure of As(V) is structurally analogous to that of Pi (Niazi et al., 2017). Roots accumulated higher As(V) as compared to the leaves probably due to (i) their close proximity to increasing As concentration in the soil solution, and (ii) GSH and PCs mediated chelation and sequestration into the vacuoles through C-type ABC transporters (Zhao et al., 2010). The higher As-accumulation in roots compared to the leaves with increasing soil arsenic levels have also been reported in *Pisum* (Rafiq et al., 2017) and *Brassica* genotypes (Niazi et al., 2017). The total As content in both roots and leaves at each As(V) treatment was comparatively lower in nitrate supplemented plants which indicates the antagonistic effect of nitrate on As(V) uptake and translocation. The decrease in arsenic content could also be correlated with (i) decrease in soil pH which results in the poor arsenic solubility, and increased sorption of As on Fe oxyhydroxides at low soil pH (Niazi et al., 2017) (ii) nitrate enhances the uptake of Pi and others nutrients that competes with As for its uptake (Singh et al., 2018c).

In leaves, sub-cellular distribution analysis revealed that arsenic was predominantly accumulated in the cell wall followed by soluble and organellar fraction The cell wall is considered as the first barrier to restrict the entry of heavy metals into cells and higher As(V) accumulation in cell wall suggests an efficient way to prevent its accumulation in the cytoplasm and organelles (Farooq et al., 2016). Moreover, biomolecules such as cellulose, hemicellulose, pectin, and proteins present in the cell wall may restrict arsenic transportation beyond the cell wall. Nitrate supplementation under As(V) toxicity caused substantial

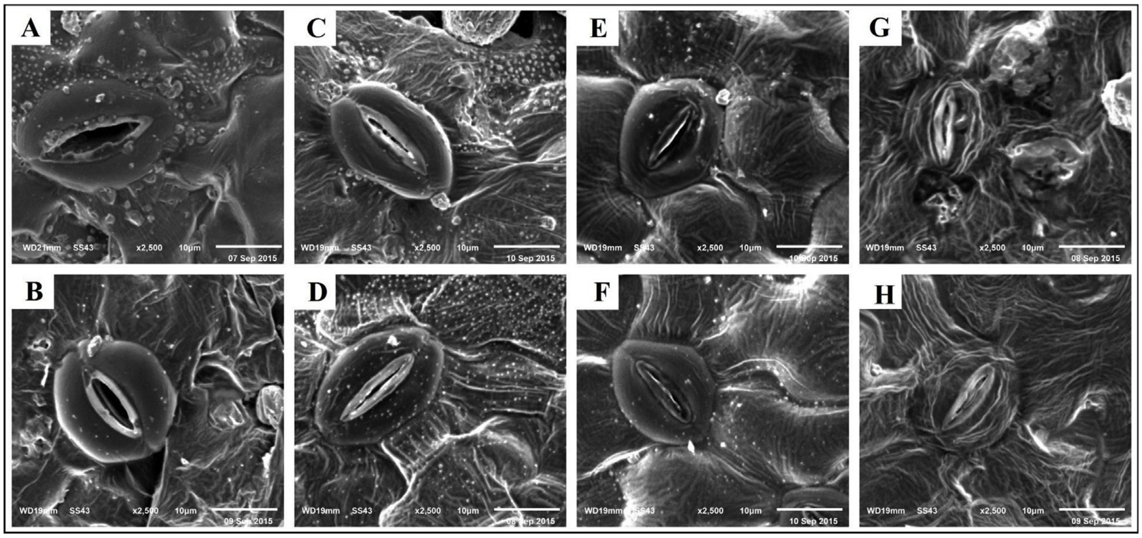

Fig. 3. Scanning electron micrographs of abaxial leaf surface of 30 days old *Solanum lycopersicum* L. showing the reduced stomatal aperture along with abnormal epidermal and guard cells at various As(V) treatments set but recovered up to the certain extent at each nitrate counterparts. (A = Control, B = 20 mM nitrate, C = 2.5 As(V), D = 2.5 As(V) + 20 mM nitrate, E = 6.25 As(V), F = 6.25 As(V) + 20 mM nitrate, G = 12.5 As(V), H = 12.5 As(V) + 20 mM nitrate). The images were taken at 2500× magnification.

reduction in the As(V) accumulation in each sub-cellular fraction compared to As(V) alone counterparts. This could be attributed to the enhanced synthesis of GSH followed by thiolation and sequestration of As into the vacuole via As(III)-(GS)$_3$] transporter proteins (Zhao et al., 2010; Abbas et al., 2018).

Exposure of tomato plants to different concentrations of As(V) resulted in the accumulation of H_2O_2 and MDA in a dose-dependent manner (Fig. 1A and B). The enhanced production of H_2O_2 might be due to the disturbances in redox homeostasis and dismutation of superoxide free radicals into H_2O_2, which, in turn, reacts with unsaturated fatty acids of membrane lipids and produces toxic lipid peroxides (MDA). MDA readily forms conjugates with membrane lipids, proteins, and nucleic acids and causes irreversible damages to the cells (Farooq et al., 2016). The results are in agreement with the studies of Singh et al. (2016a) and Rafiq et al. (2017), who also reported the increase in H_2O_2 and MDA accumulation in *Oryza sativa* and *Pisum satiuvum,* respectively, under As-toxicity. The decrease in H_2O_2 and MDA content upon nitrate supplementation could be attributed to hindrance in As(V) uptake in root cells, and increase in both enzymatic and non-enzymatic antioxidants (Zhang et al., 2014; Mehmood et al., 2017). The fall in MDA and H_2O_2 upon nitrate supplementation have also been reported by Zhang et al. (2014) in *Populus* under Cd stress.

DNA is the cell's genetic material and any damage to it leads to the malfunctioning or inactivation of the encoded proteins involved in photosynthesis, nitrogen metabolism, and AsA-GSH cycle. In order to understand the role of nitrate in alleviating the As(V) induced genotoxicity, comet assay was performed. The results showed substantial enhancements in the comet tail length and olive tail moment which can be correlated with excess H_2O_2 and MDA production under As(V) exposure. The increase in DNA damage under As(V) toxicity could be attributed to the (i) oxidative base damage via formation of DNA-protein adducts, (ii) chromosome breaks, (iii) generation of apyrimidinic/apurinic sites, and (iv) inactivation of DNA repair enzymes by limiting the ATP availability (Chandrakar et al., 2017; Abbas et al., 2018). It has been reported that arsenic-aggravates DNA damage in *Glycine max* by increasing the DNA oxidation, DNA fragmentation, and DNase activity

Table 3
Carbonic anhydrase activity, starch and sucrose content in leaves of *Solanum lycopersicum* L. grown under various As(V) treatments and 20 mM nitrate supplementation. Data is presented as mean ± S.E (n = 3). Different lower case letters indicate significant differences among the treatments as per Duncan's test.

Treatments	Carbonic anhydrase activity (Unit g^{-1} FW)	Starch content (mg g^{-1} FW)	Sucrose content (mg g^{-1} FW)
Control	99.60 ± 7.36^{a,b}	154.17 ± 19.09^{b}	38.00 ± 0.71^{c}
NO_3^-	109.24 ± 14.11^{a}	187.5 ± 12.5^{a}	42.67 ± 1.61^{b}
2.5 As(V)	87.55 ± 5.02^{b,c}	125.00 ± 12.5^{c,d}	42.67 ± 3.75^{b}
2.5 As(V) + NO_3^-	92.37 ± 3.68^{b}	133.33 ± 14.43^{b,c,d}	50.83 ± 3.62^{a}
6.25 As(V)	63.45 ± 6.06^{d,e}	108.33 ± 7.22^{d,e}	17.67 ± 1.04^{d}
6.25 As(V) + NO_3^-	76.31 ± 6.06^{c,d}	141.67 ± 7.22^{b,c}	23.00 ± 3.28^{e}
12.5 As(V)	48.19 ± 6.38^{f}	95.83 ± 14.43^{e}	12.33 ± 1.04^{f}
12.5 As(V) + NO_3^-	57.03 ± 8.46^{e,f}	108.33 ± 19.09^{d,e}	13.92 ± 0.95^{e,f}

Table 2
Net photosynthetic rate (A), stomatal conductance (G_{H2O}), chlorophyll fluorescence (F_v/F_m) and contents of chlorophyll *a,* chlorophyll *b* and carotenoids in *Solanum lycopersicum* L. grown under various As(V) treatments and 20 mM nitrate supplementation. Data is presented as mean ± S.E (n = 3). Different lower case letters indicate significant differences among the treatments as per Duncan's test.

Treatments	A (μmol CO2 m^{-2} s^{-1})	GH_2O (mmol H_2O m^{-2} s^{-1})	F_v/F_m	Chlorophyll *a* (mg g^{-1} FW)	Chlorophyll *b* (mg g^{-1} FW)	Carotenoids (mg g^{-1} FW)
Control	17.12 ± 0.05^{b}	516.87 ± 0.18^{a}	0.78 ± 0.0010^{d}	0.83 ± 0.025^{b}	0.50 ± 0.015^{b}	0.57 ± .005^{b}
NO_3^-	18.18 ± 0.13^{a}	520.50 ± 0.48^{a}	0.81 ± 0.0023^{a}	1.03 ± 0.015^{a}	0.62 ± 0.008^{f}	0.70 ± .007^{a}
2.5 As(V)	14.53 ± 0.42^{d}	412.81 ± 6.09^{e}	0.72 ± 0.0032^{d}	0.51 ± 0.031^{c}	0.31 ± 0.019^{c}	0.29 ± 0.068^{d,e}
2.5 As(V) + NO_3^-	16.02 ± 0.01^{c}	520.65 ± 0.30^{a}	0.80 ± 0.0017^{c}	0.81 ± 0.014^{b}	0.49 ± 0.007^{b}	0.57 ± 0.005^{b}
6.25 As(V)	9.40 ± 0.28^{g}	463.71 ± 3.12^{d}	0.75 ± 0.006^{g}	0.43 ± 0.013^{d}	0.26 ± 0.008^{d}	0.31 ± 0.010^{c,d}
6.25 As(V) + NO_3^-	11.13 ± 0.11^{e}	503.22 ± 2.36^{b}	0.79 ± 0.0047^{c}	0.49 ± 0.014^{c}	0.30 ± 0.008^{c}	0.35 ± 0.010^{c}
12.5 As(V)	8.46 ± 0.13^{h}	336.32 ± 4.15^{f}	0.68 ± 0.0016^{h}	0.26 ± 0.004^{e}	0.15 ± 0.002^{f}	0.19 ± 0.006^{f}
12.5 As(V) + NO_3^-	10.21 ± 0.04^{f}	488.16 ± 2.41^{c}	0.70 ± 0.0021^{g}	0.35 ± 0.006^{f}	0.21 ± 0.003^{e}	0.26 ± 0.008^{e}

Table 4
Inorganic nitrogen (nitrate, nitrite and ammonium) content in leaves of *Solanum lycopersicum* L. grown under various As(V) treatments and 20 mM nitrate supplementation. Data is presented as mean ± S.E (n = 3). Different lower case letters indicate significant differences among the treatments as per Duncan's test.

Treatments	Inorganic nitrogen contents (µg g^{-1} DW)		
	Nitrate content	Nitrite content	Ammonium
Control	1503.57 ± 61.37^b	733.47 ± $66.68^{b,c}$	287.74 ± 5.15^b
NO_3^-	1677.48 ± 17.72^a	977.96 ± 76.99^a	324.84 ± 11.84^a
2.5 As(V)	1186.49 ± 35.43^c	622.34 ± 38.50^d	250.65 ± 10.84^c
2.5 As(V) + NO_3^-	1247.86 ± 35.43^c	811.26 ± 50.93^b	284.37 ± 5.15^b
6.25 As(V)	859.18 ± 61.37^e	411.19 ± 83.90^e	213.56 ± 10.30^d
6.25 As(V) + NO_3^-	1043.29 ± 30.69^d	644.56 ± $38.50^{c,d}$	240.54 ± 1.95^c
12.5 As(V)	797.81 ± 30.69^e	300.06 ± 33.34^f	171.97 ± 5.84^e
12.5 As(V) + NO_3^-	838.72 ± 35.43^e	466.75 ± 66.68^e	209.06 ± 8.92^d

(Chandrakar et al., 2017). Nitrate mediated decrease in TL and OTM values under As(V) toxicity could be due to (i) limitation in the uptake of As from the soil, (ii) overproduction of metal chelators i.e. GSH and PCs, and sequestration of As-chelators complex into the vacuole, and (iii) scavenging of excess ROS as nitrate increases both enzymatic and non-enzymatic antioxidants (Zhang et al., 2014; Zhong et al., 2018a), and (iv) involvement of nitrogen in the synthesis of DNA base pairs (Krapp, 2015).

5.2. Photosynthetic performance under As(V) exposure and nitrate supplementation

As(V) treated plants showed abnormal, dysfunctional and closed stomata with distorted guard cells (Fig. 3). It has been reported that the differentiation and development of guard cells are mediated through the appearance of microtubules at a specific time and locations (Gupta and Bhatnagar, 2015). The anomalies in the stomatal shape could be attributed to the failure of microtubules assembly due to their interaction with As. The direct involvement of ABA in stomatal closure and subsequent reduction in water loss and CO_2 availability have been reported in Soybean under As toxicity (Armendariz et al., 2016). In the present study, nitrate mediated enhancement in the stomatal opening is in agreement to Zhong et al. (2018b) who also reported the positive role of nitrate in enhancing the stomatal opening by depolarizing the guard cells under the stress conditions.

The leaf gaseous exchange parameters (A and GH_2O) and chlorophyll fluorescence (F_v/F_m) were declined in a concentration-dependent manner with increasing As(V) in the soil. As(V) induced stomatal closure disturbed the H_2O/CO_2 gas exchanges which further limit the A and GH_2O (Armendariz et al., 2016; Singh et al., 2018c). However, the direct effects of As on thylakoid membranes and different components of light reactions are responsible for the inhibition in F_v/F_m (Farooq et al., 2016). Earlier, arsenic is reported to decrease the net photosynthesis and stomatal conductance in *Brassica* (Farooq et al., 2016; Niazi et al., 2017), and *Zea mays* (Mehmood et al., 2017; Anjum et al., 2017). Nitrate supplementation improved the A, GH_2O, and F_v/F_m as

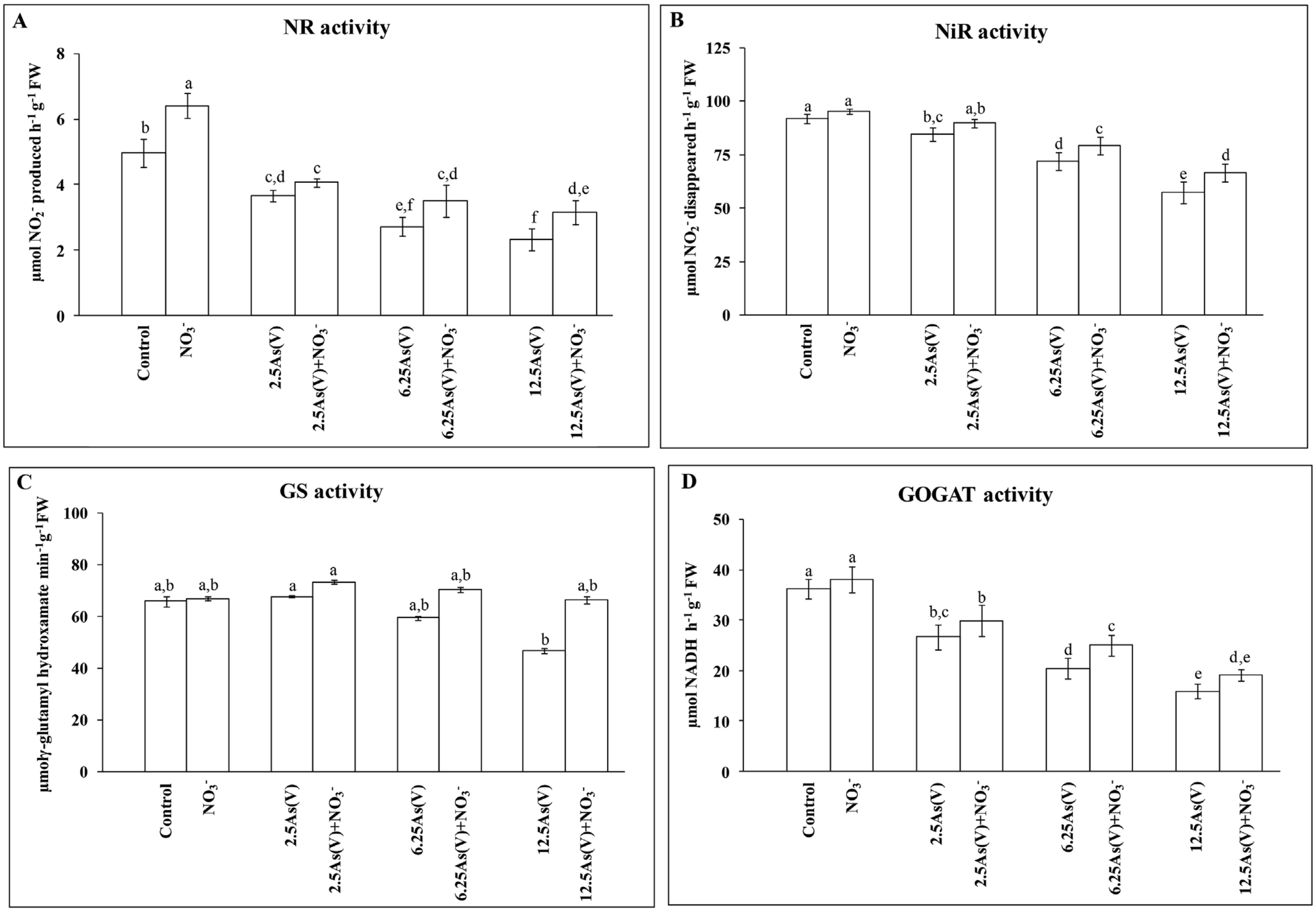

Fig. 4. Leaf nitrogen assimilating enzymes activities (A) nitrate reductase (NR), (B) nitrite reductase (NiR), (C) glutamine synthetase (GS), and (D) glutamate oxoglutarate amino transferase (GOGAT) in *Solanum lycopersicum* L. grown under various As(V) treatments and 20 mM nitrate supplementation. Data is presented as mean ± S.E (n = 3). Different lower case letters indicate significant differences among the treatments as per Duncan's test.

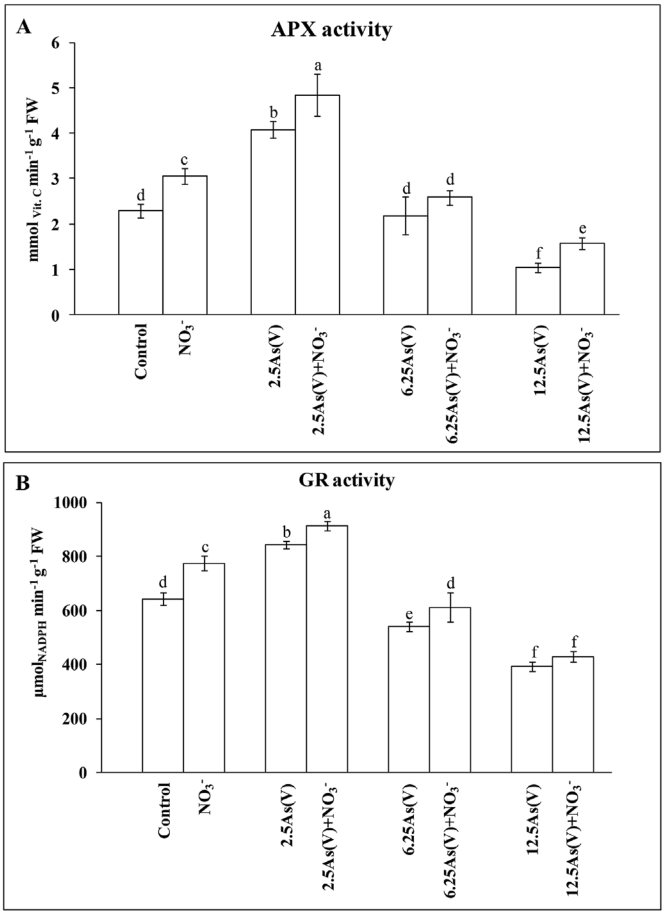

Fig. 5. Antioxidant enzymes (A) ascorbate peroxidase (APX), and (B) glutathione reductase (GR) activities in leaves of *Solanum lycopersicum* L. grown under various As(V) treatments and 20 mM nitrate supplementation. Data is presented as mean ± S.E (n = 3). Different lower case letters indicate significant differences among the treatments as per Duncan's test.

evidenced by the increase in their values as compared to their As(V) alone counterparts. This could be due to the recovery of stomatal integrity, which, in turn, facilitates the H_2O/CO_2 gas exchanges. It is reported that nitrate mediated enhancement in N metabolism can consume excessive energy (ATP) and reducing power [NAD(P)H], which, in turn, partly dissipates the excessive captured light energy to mitigate the photoinhibition of photosynthesis under the stress conditions (Singh et al., 2018c). The nitrogen mediated enhancement of photosynthesis along with coordinated regulation of carbon and nitrogen metabolism have also been reported in *Oryza sativa* under short-term water stress (Zhong et al., 2018b).

Photosynthetic pigments are important indicators to assess the photosynthetic performance of plants under normal and stress conditions. The decline in photosynthetic pigments under As(V) toxicity might be linked to hindrance in the uptake of essential nutrients, inhibition in aminolevulinic acid and protochlorophyll reductase, and degradation of chlorophyll by increasing chlorophyllase activity (Anjum et al., 2017). The increase in photosynthetic pigments by nitrate supplementation could be correlated with the stimulating effects on pigments biosynthesis as reported in *Populus* plants subjected to cadmium stress (Zhang et al., 2014).

Carbonic anhydrase (CA) catalyzes the reversible interconversion of CO_2 and HCO_3^- and facilitates the CO_2 supply to Rubisco in the C_3 plants and to PEPCase in C_4 plants. The inhibition in CA activity was probably due to hindered Zn uptake, which is an important component of its active site (Singh et al., 2016b) and decreased internal CO_2 concentration due to the stomatal closure. However, under nitrate supplementation the increase in CA activity attributed to the enhancement in the stomatal opening, which eases the CO_2 availability in the leaf. (Singh et al., 2016c; Zhong et al., 2017). The photosynthates (sucrose, starch) production represent the coordinated function of A, GH_2O, F_v/F_m, photosynthetic pigments, and carbonic anhydrase under stress and normal conditions. The decrease in photosynthates contents under As(V) exposure could result due to perturbations in gaseous exchange, photosynthetic pigments biosynthesis, and carbonic anhydrase activity. Contrarily, the enhancement in both starch and sucrose contents upon nitrate supplementation could be due to increased activities of sucrose phosphate synthetase (SPS), hexokinase (HXK), and glyceraldehyde-3-phosphate dehydrogenase (GAPDH) as reported in *Oryza sativa* under nitrogen application and moderate water deficit stress (Zhong et al., 2018a).

5.3. Nitrogen assimilation under As(V) exposure and nitrate supplementation

Nitrogen is an essential nutrient and considered to be an integral part of proteins, enzymes, chlorophyll, and nucleic acids that are crucial for photosynthesis and nitrogen assimilation (Krapp, 2015). Hence, the impact of As(V) toxicity on NO_3^-, NO_2^-, and NH_4^+ contents along with different enzymes involved in nitrogen assimilation was studied. The results showed that NO_3^-, NO_2^-, and NH_4^+ contents were decreased with increasing As(V) concentrations in the soil. The decline in NO_3^- content could be attributed to (i) As-induced stomatal closure, which decreased the transpiration (Niazi et al., 2017) and lowers the NO_3^- flux from root to shoot via xylem, (ii) generation of excess ROS that disturbs the membrane integrity and hinders the uptake of NO_3^- by nitrate transporters (Singh et al., 2018c). The decrease in NO_2^- and NH_4^+ contents could directly be linked with limited NO_3^- supply and inhibition in NR and NiR activities (Table 4; Fig. 4A and B). Nitrate supplementation increased the NO_3^-, NO_2^-, and NH_4^+ contents as it (i) promotes stomatal opening and transpiration for efficient nitrate uptake, (ii) maintains membrane integrity by increasing the ROS scavenging enzymes activities, and (iii) enhances the NR and NiR

Table 5

Contents of ascorbate (AsA), dehydroascorbate (DHA), reduced glutathione(GSH), oxidized glutathione(GSSG) and ratios' of AsA/DHA, and GSH/GSSG in leaves of *Solanum lycopersicum* L. grown under various As(V) treatments and 20 mM nitrate supplementation. Data is presented as mean ± S.E (n = 3). Different lower case letters indicate significant differences among the treatments as per Duncan's test.

Treatments	AsA (µ mol g^{-1} FW)	DHA (µ mol g^{-1} FW)	AsA/DHA	GSH (µ mol g^{-1} FW)	GSSG (µ mol g^{-1} FW)	GSH/GSSG
Control	18.95 ± 1.30^{c}	12.49 ± 2.13^{a}	$1.55 \pm 0.32^{d,e}$	3.47 ± 0.22^{e}	1.76 ± 0.1^{a}	$1.98 \pm 0.23^{b,c,d}$
NO_3^-	25.82 ± 1.59^{b}	$11.09 \pm 1.12^{a,b}$	2.35 ± 0.31^{c}	4.05 ± 0.26^{d}	$1.98 \pm 0.02^{a,b,c}$	$2.04 \pm 0.15^{a,b}$
2.5 As(V)	28.00 ± 1.01^{b}	13.64 ± 2.16^{a}	$2.08 \pm 0.31^{c,d}$	5.60 ± 0.27^{b}	$2.27 \pm 0.31^{a,b}$	$2.51 \pm 0.43^{a,b}$
2.5 As(V) + NO_3^-	33.83 ± 1.04^{a}	7.39 ± 0.29^{c}	4.58 ± 0.04^{a}	6.75 ± 0.18^{a}	2.42 ± 0.34^{a}	2.80 ± 0.5^{a}
6.25 As(V)	21.20 ± 1.73^{c}	12.52 ± 2.51^{a}	$1.72 \pm 0.20^{c,d,e}$	4.62 ± 0.27^{c}	$1.78 \pm 0.1^{b,c}$	$2.60 \pm 0.17^{a,b}$
6.25 As(V) + NO_3^-	27.99 ± 1.71^{b}	$9.06 \pm 1.20^{b,c}$	3.15 ± 0.62^{b}	5.54 ± 0.39^{b}	$2.00 \pm 0.1^{a,b,c}$	2.76 ± 0.12^{a}
12.5 As(V)	12.60 ± 1.18^{d}	$11.38 \pm 2.11^{a,b}$	1.15 ± 0.33^{e}	2.26 ± 0.27^{g}	1.68 ± 0.33^{c}	1.39 ± 0.38^{d}
12.5 As(V) + NO_3^-	15.68 ± 0.52^{e}	$9.66 \pm 1.13^{b,c}$	$1.88 \pm 0.38^{c,d}$	2.77 ± 0.17^{f}	$1.89 \pm 0.43^{b,c}$	$1.53 \pm 0.4^{c,d}$

Table 6
Two-way ANOVA analysis reveals the effects of As(V), nitrate, and their interactions on arsenic contents, photosynthesis, nitrogen metabolism, AsA-GSH cycle, toxicity indices, and DNA damage in *Solanum lycopersicum* L. Data represent the values of F and P and the significance level is $\leq$ *0.05*.

	Arsenic (V)	Nitrate	Arsenic × Nitrate
1. Arsenic contents			
Cell wall (F1)	F = 299.52, P = 0.000	F = 110.21, P = 0.000	F = 30.35, P = 0.000
Soluble (F2)	F = 839.92, P = 0.000	F = 754.20, P = 0.000	F = 100.34, P = 0.000
Organelles (F3)	F = 173.91, P = 0.000	F = 61.44, P = 0.000	F = 12.69, P = 0.000
Root	F = 554.65, P = 0.000	F = 7343.72, P = 0.000	F = 887.01, P = 0.000
Leaf	F = 2238.60, P = 0.000	F = 594.41, P = 0.000	F = 87.49, P = 0.000
2. Toxicity Indices			
H2O2 content	F = 148.74, P = 0.000	F = 9.69, P = 0.007	F = 0.69, P = 0.571
MDA content	F = 2117.78, P = 0.000	F = 256.97, P = 0.000	F = 64.46, P = 0.000
3. DNA damage			
Tail length	F = 98.01, P = 0.000	F = 60.69, P = 0.000	F = 26.85, P = 0.000
Olive tail moment	F = 265.91, P = 0.000	F = 204.24, P = 0.000	F = 139.83, P = 0.000
4. Photosynthesis			
Net photosynthetic rate	F = 2507.82, P = 0.000	F = 360.02, P = 0.000	F = 4.01, P = 0.026
Stomatal conductance	F = 1148.02, P = 0.000	F = 3629.61, P = 0.000	F = 800.55, P = 0.000
Fv/Fm	F = 2126.05, P = 0.000	F = 1667.23, P = 0.000	F = 159.41, P = 0.000
Chlorophyll *a*	F = 1430.62, P = 0.000	F = 523.82, P = 0.000	F = 57.67, P = 0.000
Chlorophyll b	F = 1533.73, P = 0.000	F = 557.02, P = 0.000	F = 62.57, P = 0.000
Carotenoids	F = 291.68, P = 0.000	F = 156.23, P = 0.000	F = 25.17, P = 0.000
CA activity	F = 51.73, P = 0.000	F = 8.20, P = 0.000	F = 0.27, P = 0.843
Starch	F = 25.19, P = 0.000	F = 14.70, P = 0.001	F = 1.38, P = 0.289
Sucrose	F = 258.21, P = 0.000	F = 6.52, P = 0.021	F = 8.92, P = 0.001
5. N-metabolism			
Nitrate content	F = 412.55, P = 0.000	F = 47.093, P = 0.000	F = 4.922, P = 0.013
Nitrite content	F = 225.19, P = 0.000	F = 102.13, P = 0.000	F = 0.51, P = 0.681
Ammonium content	F = 72.57 P = 0.000	F = 73.05, P = 0.000	F = 0.57, P = 0.645
NR activity	F = 87.47, P = 0.000	F = 38.56, P = 0.000	F = 2.34, P = 0.111
NiR activity	F = 98.52, P = 0.000	F = 20.34, P = 0.000	F = 0.85, P = 0.489
GS activity	F = 162.94, P = 0.000	F = 407.92, P = 0.000	F = 75.53, P = 0.000
GOGAT activity	F = 90.79, P = 0.000	F = 13.79, P = 0.002	F = 0.37, P = 0.777
6. AsA-GSH cycle			
AsA content	F = 165.88, P = 0.000	F = 109.99, P = 0.000	F = 2.72, P = 0.079
DHA content	F = 1.129, P = 0.367	F = 23.52, P = 0.000	F = 1.99, P = 0.156
AsA/DHA ratio	F = 29.87, P = 0.000	F = 91.26, P = 0.000	F = 8.19, P = 0.002
GSH content	F = 224.29, P = 0.000	F = 55.03, P = 0.000	F = 1.96, P = 0.160
GSSG content	F = 5.81, P = 0.007	F = 3.79, P = 0.069	F = 0.009, P = 0.999
GSH/GSSG ratio	F = 19.00, P = 0.000	F = 1.49, P = 0.240	F = 0.134, P = 0.939
APX activity	F = 157.84, P = 0.000	F = 34.72, P = 0.000	F = 0.75, P = 0.538
GR activity	F = 329.77, P = 0.000	F = 51.04, P = 0.000	F = 3.34, P = 0.046

activities.

Nitrate reductase is a rate-limiting enzyme in nitrogen assimilation and is highly sensitive to heavy metal toxicity (Singh et al., 2009). The decrease in NR activity might be due to the direct inhibitory effects of arsenic on the enzyme synthesis and/or activity. Since sulfhydryl (−SH) groups are critical for NADH binding and catalytic activity of NR, arsenic might also affect the NR activity by reacting with functional −SH groups present in the active sites (Abbas et al., 2018; Singh et al., 2018c). In addition, NR has been demonstrated to be sensitive to H_2O_2 (Singh et al., 2009), therefore enhancement in the H_2O_2 content could be responsible for lowered NR activity. The damages in the photosynthetic electron transport chain can affect the NiR activity as it donates electrons for NO_2^- reduction via ferredoxin. Also, the decline in NO_3^- and NO_2^- contents in the cell's interior under arsenic exposure might have resulted in the decreased NR and NiR activity. The GS/GOGAT cycle incorporates ammonium ions into glutamate, which is used for biosynthesis of several other amino acids. The decreased GS and GOGAT activities were probably due to (i) oxidative modifications of these enzymes by excess ROS (Singh et al., 2018c), and (ii) limitation in the substrate NH_4^+ due to lowered NO_3^- and NO_2^- availability. Previously, As-induced decreases in NR, NiR, GS and GOGAT activities were reported in *Brassica juncea* (Singh et al., 2018c) and similar results were obtained for NR and NiR activities in *Pteris vittata* under different levels of arsenic stress (Singh et al., 2009). Nitrate supplementation resulted in higher NR, NiR, GS and GOGAT activities as compared to their As(V) alone counterparts. This improvement could be achieved due to enhanced availability of nitrate which is the prerequisite for nitrogen metabolism (Krapp, 2015). The nitrogen mediated enhancements of NR, NiR, GS and GOGAT activities were also reported in tomato (Singh et al., 2016b) under salinity stress, and rice (Zhong et al., 2018a) under moderate water deficit stress.

5.4. Ascorbate-glutathione cycle under As(V) exposure and nitrate supplementation

The AsA-GSH cycle is crucial to maintain the cellular redox homeostasis under stress conditions and consequently alleviates the lipid peroxidation, DNA damage, photosynthesis and nitrogen metabolism (Chandrakar et al., 2017; Farooq et al., 2018; Zhong et al., 2018a). The AsA-GSH cycle efficiently detoxifies H_2O_2, and enzymes such as APX and GR are crucial to the cycle (Noctor et al., 2016). The APX directly scavenges the H_2O_2 and GR maintains a high GSH/GSSG ratio required for the regeneration of AsA. The activities of APX and GR were increased at 2.5 As(V), while decreased at 6.25 and 12.5 As(V) treatments (Fig. 5A and B). The increased activity of both enzymes at 2.5 As(V) indicates the signalling behavior of free radicals in the induction of the transcription of their genes (Farooq et al., 2016). Contrarily, the loss in APX and GR activities at 6.25, and 12.5 As(V) treatments could have occurred due to (i) inhibition in the uptake of essential nutrients and sensitivity of thiol groups at their active sites to heavy metals (Singh et al., 2018c) (ii) inactivation by excess H_2O_2, and (iv) inhibition at transcription and translation levels (Farooq et al., 2016). Nitrate supplementation boosts APX and GR activity effectively at each respective As(V) treatments probably due to up-regulation of the gene expression to create more antioxidant enzymes (Zhang et al., 2014). Nitrate reductase-dependent nitric oxide (NO) biosynthesis is well documented in plants. In this study, nitrate supplementation increases the NR activity and thus, improved performance of AsA-GSH cycle may indirectly be linked to the enhanced NO biosynthesis, which is well-reported abiotic-stress modulator in plants (Singh et al., 2016a). The nitrate mediated enhancement in APX activity is also reported in *Populus* under Cd stress (Zhang et al., 2014), and in APX and GR in *Brassica juncea* under arsenic stress (Singh et al., 2018c).

Ascorbate and glutathione are two important redox buffering agents that protect the plasma membrane from oxidation. Ascorbate is an effective ROS scavenger while GSH is critical for sequestration of HMs to the vacuoles (Farooq et al., 2018). AsA/DHA and GSH/GSSG ratios reflect redox status of the cell and their high ratios are crucial for plant survival under the stress conditions. In this study, the contents of AsA, DHA and AsA/DHA ratio were increased at 2.5 and 6.25 As(V), while decreased at 12.5 As(V) treatment as compared to the control; similar results were obtained for GSH, GSSG and GSH/GSSG ratio. The decline in the AsA content, and AsA/DHA ratio at the highest As(V) treatment attributed to its consumption for quenching ROS. However, decreased GSH content, and GSH/GSSG ratio probably occurred due to (i) increased consumption in the biosynthesis of phytochelatins (Seth et al., 2012), (ii) decreased GR activity resulting in less GSH regeneration from GSSG, and (iii) its consumption in several cellular metabolic processes as it acts as a central defense molecule (Seth et al., 2012; Farooq et al., 2018). Earlier studies also reported the decline in GSH content in *Helianthus annus* under As stress (Azeem et al., 2017), ratios of AsA/DHA, and GSH/GSSG in *Ozyza sativa* L. under Cd (Rahman et al., 2016) stress. Nitrate supplementation improved the contents of AsA, GSH, and ratios of AsA/DHA, GSH/GSSG at each of their respective As(V) alone treatments. The enhancement in GSH could be due to the upregulation of γ-glutamine cysteine synthetase (*gsh1*) and glutathione synthetase (*gsh2*) as reported in *Arabidopsis* under Cd exposure (Xiang and Oliver, 1998). Further, the enhanced GSH is responsible for efficient AsA regeneration and maintaining the AsA pool and AsA/DHA ratio.

6. Conclusions

The present study concludes that As(V) stress hampered the plant growth by interfering with two key metabolic processes *viz.* photosynthesis and nitrogen assimilation as obvious from higher As-accumulation in root, leaf and leaf sub-cellular fractions. Nitrate supplementation ameliorates As(V) toxicity through boosting the performance of the AsA-GSH cycle, which curbs the lipid peroxidation and DNA damage. The efficient AsA-GSH cycle also maintains the cellular redox homeostasis and thereby improves the overall plant growth by enhancing the photosynthetic performance and nitrogen assimilation. This study lays a platform to elucidate the molecular mechanism(s) of nitrate mediated alleviation of As(V) toxicity in plants by examining the responsive genes and transporters proteins involved in As-speciation, accumulation and vacuolar sequestration.

Declaration of conflict of interest

All the authors have no conflict of interest.

Authors' contribution

Praveen Gupta: Performing, collection and assembly of the data, analysis, and interpretation of the data, drafting and writing the manuscript, statistical analysis. Chandra Shekhar Seth: Conception and design of the experiment, critical revision of the article for important intellectual content, final approval of the article, provision of study materials, experimental expertise, obtaining of funding, administrative, technical, or logistic support

Acknowledgments

Dr. C.S. Seth is thankful to the University of Delhi for providing Research and Development Grant vide reference number RC/2015/9677, and Department of Science and Technology, New Delhi for granting the DST-DU-Purse Grant. Mr. Praveen Gupta is thankful to the UGC for awarding the Junior Research Fellowship. The technical staffs in the central instrumentation facility, Department of Botany are also acknowledged for their constant support. Prof. MNV Prasad, University of Hyderabad, India is acknowledged for his critical editing and scientific suggestions in this manuscript.

References

Abbas, G., Murtaza, B., Bibi, I., Shahid, M., Niazi, N.K., Khan, M.I., Amjad, M., Hussain, M., 2018. Arsenic uptake, toxicity, detoxification, and speciation in plants: physiological, biochemical, and molecular aspects. Int. J. Environ. Res. Public Health 15, 59. https://doi.org/10.3390/ijerph15010059.

Alexieva, V., Sergiev, I., Mapelli, S., Karanov, E., 2001. The effect of drought and ultraviolet radiation on growth and stress markers in pea and wheat. Plant Cell Environ. 24, 1337–1344. https://doi.org/10.1046/j.1365-3040.2001.00778.x.

Anjum, S.A., Tanveer, M., Hussain, S., Ashraf, U., Khan, I., Wang, L., 2017. Alteration in growth, leaf gas exchange, and photosynthetic pigments of maize plants under combined cadmium and arsenic stress. Water Air Soil Pollut. 228, 13. https://doi.org/10.1007/s11270-016-3187-2.

Armendariz, A.L., Talano, M.A., Villasuso, A.L., Travaglia, C., Racagni, G.E., Reinoso, H., Agostini, E., 2016. Arsenic stress induces changes in lipid signalling and evokes the stomata closure in soybean. Plant Physiol. Biochem. 103, 45–52. https://doi.org/10.1016/j.plaphy.2016.02.041.

Azeem, W., Ashraf, M., Shahzad, S.M., Imtiaz, M., Akhtar, M., Rizwan, M.S., 2017. Phosphate-arsenate relations to affect arsenic concentration in plant tissues, growth, and antioxidant efficiency of sunflower (*Helianthus annuus* L.) under arsenic stress. Environ. Sci. Pollut. Res. 24, 24376–24386. https://doi.org/10.1007/s11356-017-9977-2.

Buysse, J.A.N., Merckx, R., 1993. An improved colorimetric method to quantify sugar content of plant tissue. J. Exp. Bot. 44, 1627–1629. https://doi.org/10.1093/jxb/44.10.1627.

Cataldo, D.A., Maroon, M., Schrader, L.E., Youngs, V.L., 1975. Rapid colorimetric determination of nitrate in plant tissue by nitration of salicylic acid 1. Commun. Soil Sci. Plant Anal. 6, 71–80. https://doi.org/10.1080/00103627509366547.

Chandrakar, V., Yadu, B., Meena, R.K., Dubey, A., Keshavkant, S., 2017. Arsenic- induced genotoxic responses and their amelioration by diphenylene iodonium, 24- epibrassinolide and proline in *Glycine max* L. Plant Physiol. Biochem. 112, 74–86. https://doi.org/10.1016/j.plaphy.2016.12.023.

Clegg, K.M., 1956. The application of the anthrone reagent to the estimation of starch in cereals. J. Sci. Food Agric. 7, 40–44. https://doi.org/10.1002/jsfa.2740070108.

Farooq, M.A., Gill, R.A., Ali, B., Wang, J., Islam, F., Ali, S., Zhou, W., 2016. Subcellular distribution, modulation of antioxidant and stress-related genes response to arsenic in *Brassica napus* L. Ecotoxicology 25, 350–366. https://doi.org/10.1007/s10646-015-1594-6.

Farooq, M.A., Islam, F., Yang, C., Nawaz, A., Gill, R.A., Ali, B., Song, W., Zhou, W., 2018. Methyl jasmonate alleviates arsenic-induced oxidative damage and modulates the ascorbate-glutathione cycle in oilseed rape roots. J. Plant Growth Regul. 84, 135–148. https://doi.org/10.1007/s10725-017-0327-7.

Gichner, T., Znidar, I., Wagner, E., Plewa, M., 2016. In: Dhawan, A., Anderson, D. (Eds.), The Use of Higher Plants in the Comet Assay, second ed. Royal Society of Chemistry, London, pp. 112–133. https://doi.org/10.1039/9781782622895-FP001. Issues in toxicology no. 30. The comet assay in toxicology.

Gupta, P., Bhatnagar, A.K., 2015. Spatial distribution of arsenic in different leaf tissues and its effect on structure and development of stomata and trichomes in mungbean, *Vigna radiata* (L.) Wilczek. Environ. Exp. Bot. 109, 12–22. https://doi.org/10.1016/j.envexpbot.2014.08.001.

Gupta, P., Srivastava, S., Seth, C.S., 2017. 24-Epibrassinolide and Sodium Nitroprusside alleviate the salinity stress in *Brassica juncea* L. cv. Varuna through cross talk among proline, nitrogen metabolism and abscisic acid. Plant Soil 411, 483–498. https://doi.org/10.1007/s11104-016-3043-6.

Heath, R.L., Packer, L., 1968. Photoperoxidation in isolated chloroplasts, I. Kinetics and stoichiometry of fatty acid peroxidation. Arch. Biochem. Biophys. 125, 189–198. https://doi.org/10.1016/0003-9861(68)90654-1.

Hiscox, J.D., Israelstam, G.F., 1979. A method for the extraction of chlorophyll from leaf tissue without maceration. Can. J. Bot. 57, 1332–1334. https://doi.org/10.1139/b79-163.

Krapp, A., 2015. Plant nitrogen assimilation and its regulation: a complex puzzle with missing pieces. Curr. Opin. Plant Biol. 25, 115–122. https://doi.org/10.1016/j.pbi.2015.05.010.

Mehmood, T., Bibi, I., Shahid, M., Niazi, N.K., Murtaza, B., Wang, H., Ok, Y.S., Sarkar, B., Javed, M.T., Murtaza, G., 2017. Effect of compost addition on arsenic uptake, morphological and physiological attributes of maize plants grown in contrasting soils. J. Geochem. Explor. 178, 83–91. https://doi.org/10.1016/j.gexplo.2017.03.018.

Molins-Legua, C., Meseguer-Lloret, S., Moliner-Martinez, Y., Campins-Falco, P., 2006. A guide for selecting the most appropriate method for ammonium determination in water analysis. Trends Anal. Chem. 20, 282–290. https://doi.org/10.1016/j.trac.2005.12.002.

Niazi, N.K., Bibi, I., Fatimah, A., Shahid, M., Javed, M.T., Wang, H., Ok, Y.S., Bashir, S., Murtaza, B., Saqib, Z.A., Shakoor, M.B., 2017. Phosphate-assisted phytoremediation of arsenic by *Brassica napus* and *Brassica juncea*: morphological and physiological response. Int. J. Phytoremediation 19, 670–678. https://doi.org/10.1080/15226514.2016.1278427.

Noctor, G., Mhamdi, A., Foyer, C.H., 2016. Oxidative stress and antioxidative systems: recipes for successful data collection and interpretation. Plant Cell Environ. 39, 1140–1160. https://doi.org/10.1111/pce.12726.

O'neal, D., Joy, K.W., 1973. Glutamine synthetase of pea leaves. I. Purification, stabilization, and pH optima. Arch. Biochem. Biophys. 159, 113–122. https://doi.org/10.1016/0003- 9861(73)90435-9.

Rachim, M.A., Nicholas, D.J.D., 1985. Glutamine synthetase and glutamate synthase from *Sclerotinia sclerotiorum*. Phytochemistry 24, 2451–2548. https://doi.org/10.1016/S0031- 9422(00)80664-0.

Rafiq, M., Shahid, M., Abbas, G., Shamshad, S., Khalid, S., Niazi, N.K., Dumat, C., 2017. Comparative effect of calcium and EDTA on arsenic uptake and physiological attributes of *Pisum sativum*. Int. J. Phytoremediation 19, 662–669. https://doi.org/10.1080/15226514.2016.1278426.

Rahman, A., Mostofa, M.G., Nahar, K., Hasanuzzaman, M., Fujita, M., 2016. Exogenous calcium alleviates cadmium-induced oxidative stress in rice (*Oryza sativa* L.) seedlings by regulating the antioxidant defense and glyoxalase systems. Braz. J. Bot. 39, 393–407. https://doi.org/10.1007/s40415-015-0240-0.

Sengupta, S., Shaila, M.S., 1996. Purification and characterization of assimilatory nitrite reductase from *Candida utilis*. Biochem. J. 317, 147–155. https://doi.org/10.1042/bj3170147.

Seth, C.S., Remans, T., Keunen, E., Jozefczak, M., Gielen, H., Opdenakker, K., Weyens, N., Vangronsveld, J., Cuypers, A., 2012. Phytoextraction of toxic metals: a central role for glutathione. Plant Cell Environ. 35, 334–346. https://doi.org/10.1111/j.1365-3040.2011.02338.x.

Shakoor, M.B., Niazi, N.K., Bibi, I., Murtaza, G., Kunhikrishnan, A., Seshadri, B., Shahid, M., Ali, S., Bolan, N.S., Ok, Y.S., Abid, M., 2016. Remediation of arsenic-contaminated water using agricultural wastes as biosorbents. Crit. Rev. Environ. Sci. Technol. 46, 467–499. https://doi.org/10.1080/10643389.2015.1109910.

Singh, N., Ma, L.Q., Vu, J.C., Raj, A., 2009. Effects of arsenic on nitrate metabolism in arsenic hyperaccumulating and non-hyperaccumulating ferns. Environ. Pollut. 157, 2300–2305. https://doi.org/10.1016/j.envpol.2009.03.036.

Singh, A.P., Dixit, G., Kumar, A., Mishra, S., Singh, P.K., Dwivedi, S., Trivedi, P.K., Chakrabarty, D., Mallick, S., Pandey, V., Dhankher, O.P., Tripathi, R.D., 2016a. Nitric oxide alleviated arsenic toxicity by modulation of antioxidants and thiol metabolism in rice (*Oryza sativa* L.). Front. Plant Sci. 6, 1272. https://doi.org/10.3389/fpls.2015.01272.

Singh, M., Singh, V.P., Prasad, S.M., 2016b. Responses of photosynthesis, nitrogen and proline metabolism to salinity stress in *Solanum lycopersicum* under different levels of nitrogen supplementation. Plant Physiol. Biochem. 109, 72–83. https://doi.org/10.1016/j.plaphy.2016.08.021.

Singh, R., Parihar, P., Prasad, S.M., 2018c. Sulfur and calcium simultaneously regulate photosynthetic performance and nitrogen metabolism status in As-challenged *Brassica juncea* L. seedlings. Front. Plant Sci. 9, 772. https://doi.org/10.3389/fpls.2018.00772.

Varner, J., Bulen, W., Vanecko, S., Burrell, R., 1953. Determination of ammonium, amide, nitrite, and nitrate nitrogen in plant extracts. Anal. Biochem. 25, 1528–1529. https://doi.org/10.1021/ac60082a031.

Wu, Q.S., Zou, Y.N., Xia, R.X., 2006. Effects of water stress and arbuscular mycorrhizal fungi on reactive oxygen metabolism and antioxidant production by citrus (*Citru stangerine*) roots. Eur. J. Soil Biol. 42, 166–172. https://doi.org/10.1016/j.ejsobi.2005.12.006.

Xiang, C.B., Oliver, D.J., 1998. Glutathione metabolic genes coordinately respond to heavy metals and jasmonic acid in *Arabidopsis*. Plant Cell 10, 1539–1550. https://doi.org/10.1105/tpc.10.9.1539.

Zhang, F., Wan, X., Zheng, Y., Sun, L., Chen, Q., Zhu, X., Guo, Y., Liu, M., 2014. Effects of nitrogen on the activity of antioxidant enzymes and gene expression in leaves of *Populus* plants subjected to cadmium stress. J. Plant Interact. 9 (1), 599–609. https://doi.org/10.1080/17429145.2013.879676.

Zhao, F.J., McGrath, S.P., Meharg, A.A., 2010. Arsenic as a food chain contaminant, mechanisms of plant uptake and metabolism and mitigation strategies. Annu. Rev. Plant Biol. 61, 535–559. https://doi.org/10.1146/annurev-arplant-042809-112152.

Zhong, C., Cao, X., Hu, J., Zhu, L., Zhang, J., Huang, J., Jin, Q., 2017. Nitrogen metabolism in adaptation of photosynthesis to water stress in rice grown under different nitrogen levels. Front. Plant Sci. 8, 1079. https://doi.org/10.3389/fpls.2017.01079.

Zhong, C., Bai, Z.G., Zhu, L.F., Zhang, J.H., Zhu, C.Q., Huang, J.L., Jin, Q.Y., Cao, X.C., 2018a. Nitrogen-mediated alleviation of photosynthetic inhibition under moderate water deficit stress in rice (*Oryza sativa* L.). Environ. Exp. Bot. 125, 52–62. https://doi.org/10.1016/j.envexpbot.2018.10.021.

Zhong, C., Cao, X., Bai, Z., Zhang, J., Zhu, L., Huang, J., Jin, Q., 2018b. Nitrogen metabolism correlates with the acclimation of photosynthesis to short-term water stress in rice (*Oryza sativa* L.). Plant Physiol. Biochem. 125, 52–62.